

TURBULENCE STRUCTURE LEADING TO UNSTEADY UPSTREAM SEPARATION IN COUETTE FLOW WITH FORWARD-FACING STEP

Yohei Morinishi

Graduate School of Engineering
Nagoya Institute of Technology
Gokiso-cho, Showa-ku, Nagoya, 466-8555, Japan
morinishi.yohei@nitech.ac.jp

Shohei Kubota

Graduate School of Engineering
Nagoya Institute of Technology
Gokiso-cho, Showa-ku, Nagoya, 466-8555, Japan
28413069@stn.nitech.ac.jp

Shinji Tamano

Graduate School of Engineering
Nagoya Institute of Technology
Gokiso-cho, Showa-ku, Nagoya, 466-8555, Japan
tamano.shinji@nitech.ac.jp

Toru Yamada

Graduate School of Engineering
Nagoya Institute of Technology
Gokiso-cho, Showa-ku, Nagoya, 466-8555, Japan
yamada.toru@nitech.ac.jp

ABSTRACT

The turbulence structure leading to unsteady upstream separation in a Couette flow with a forward-facing step is studied using PIV and DNS. The counter-gradient diffusion phenomenon (CDP) of the Reynolds stress appeared near the downstream separation is considered by means of conditional averaging based on the reverse flow area in the upstream separation. The negative production of the turbulence kinetic energy which is a quantitative measure of the CDP is mainly produced when the upstream separation has open form.

INTRODUCTION

Turbulent flows over a forward-facing step have considerable complexity due to acceleration, deceleration, upstream and downstream separations and reattachments, and so on. Morinishi et al (2015) studied a turbulent Couette flow with a forward-facing step using particle image velocimetry (PIV) measurement and the direct numerical simulation (DNS) of the incompressible Navier-Stokes equation. Their results indicate the counter-gradient diffusion phenomenon (CDP) of the Reynolds stress near the downstream separation. The CDP has also been observed in boundary layer flows over a forward-facing step (Hattori and Nagano, 2010). However, the CDP is hard to discuss by means of the standard ensemble averaged statistics only, since the flow over the forward-facing step is essentially unsteady.

The studies so far on the turbulence structure over a forward-facing step have mainly been focused attention on the downstream separation. On the other hand, Pearson et al. (2013) took attention on the upstream separation of the forward-facing step flow in a boundary layer. They demonstrated that the upstream separation exhibits both open and closed forms using conditional averaging based on the area of reverse flow in the upstream separation.

In this study, the turbulent structure producing the CDP of the Reynolds stress is considered experimentally and numerically in

the Couette flow with a forward-facing step by means of conditional averaging based on the area of reverse flow in the upstream separation.

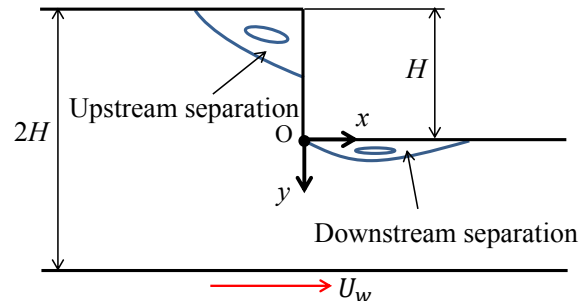


Figure 1. Schematic of the present Couette flow with a forward-facing step. In this figure, the upstream separation has open form.

EXPERIMENTAL AND NUMERICAL METHODS

Figure 1 shows the schematic of the present Couette flow with a forward-facing step. The coordinate origin is taken at the convex corner of the step. The upstream flow in the experiment is a fully developed turbulent Couette flow between lower moving and upper stationary walls with the duct aspect ratio of 21.6. The forward-facing step (step height $H = 20$ mm) on the stationary wall with contraction ratio of 0.5 is located at 3500 mm downstream of the channel inlet. The PIV measurement is conducted with double-pulse YAG laser (70 mJ/pulse) and CCD camera (1600x1200 pixels). Tracer particles for the PIV are olive oil mist (mean particle diameter is about $2 \mu\text{m}$) supplied upstream of the channel. Sampling frequency for the PIV image shooting is 10 Hz. The Reynolds number based on the step height H and the moving wall velocity U_w is $Re_w = U_w H / \nu = 3000$ where ν is the kinematic viscosity of the working fluid (air). The DNS of the

incompressible Navier-Stokes equation for the Couette flow with a forward-facing step is carried out at the same Reynolds number as the experiment. In the DNS, the equation is solved using the fully conservative second-order finite-difference method in a staggered grid and the implicit mid-point time marching method. The number of numerical grid is $230 \times 100 \times 60$ (streamwise \times wall-normal \times spanwise) in the computational region of $22H \times 2H \times 6H$. Experimental and numerical methods are basically the same as those in Morinishi et al. (2015) where the standard turbulence statistics are presented.

RESULTS AND DISCUSSIONS

Figure 2 shows the comparison between experimental and numerical results of streamwise mean velocity profiles as an example at several downstream sections. Here, the mean velocity profiles are estimated by means of standard ensemble averaging. The experimental and numerical results are in good agreement with each other which demonstrates the reliability of the DNS data. The flow accelerates toward the contraction at the forward-facing step, separates, and finally redevelops. The reverse flows close to the upper wall in the upstream and downstream regions correspond to the upstream and downstream separations, respectively.

Figure 3 shows the streamlines and negative production regions of turbulence kinetic energy computed from the DNS data. The production of turbulence kinetic energy P_k is defined as follows:

$$P_k = -\overline{u_i u_j} \frac{\partial U_i}{\partial x_j} = 2 \nu_t S_{ij} S_{ij} \quad (1)$$

The second equality substitutes the eddy viscosity hypothesis to the Reynolds stress, where ν_t and S_{ij} are the eddy viscosity and mean strain rate tensor, respectively. From this relation the negative production indicates the appearance of the CDP of the Reynolds stress (Hattori and Nagano, 2010). The negative production regions appear slightly inside the front shear layer and in the rear part of wall layer in the downstream separation. However, the CDP is hard to discuss by means of the standard ensemble averaged statistics only, since the flow over the forward-facing step is considerably unsteady.

Figure 4 shows the distributions of probability density function (PDF) of reverse flow area A in the upstream separation computed from PIV and DNS data. The reverse flow area is defined as the sum of areas where the streamwise velocity component has negative sign in the region upstream of the forward-facing step. The PDF distributions from PIV and DNS data are qualitatively in good agreement with each other. The distributions of the PDF are asymmetric about the peak locations between $A/H^2 = 0.1$ and 0.2 . In addition, the upstream separation has open form when $A/H^2 \leq 0.4$, while it has closed form when $A/H^2 \geq 0.5$, which is consistent with the observation by Pearson et al. (2013). From the PDF distribution and the critical value of the reverse flow area, it is understood that the open form separation is dominant in the present flow, while the closed form separation appears intermittently.

Figure 5 shows the examples of open and closed forms of the separation which are derived from the conditional averaging

based on the upstream reverse flow area. The open form separation (Fig.5(a)) reattaches on the forward-facing step, while the closed form separation (Fig.5(b)) gets over the step corner and encloses the downstream separation.

Figure 6 shows the time history of the upstream reverse flow area A at some spanwise sections. We can specify periods in which the open and closed form separations are respectively dominant. Figure 7 shows coherent vortex structures visualized by the second invariant of velocity gradient tensor, $Q_2 H^2 / U_w^2 = 1.0$. Elongated coherent vortex structures get over the step corner at the period of closed form separation (Fig. 7(b), $U_w t/H = 350$), while such behaviour does not observed at the period of open form separation (Fig. 7(a), $U_w t/H = 314$). The result reveals the apparent difference of flow structures between the periods of open and closed form separations.

Then, the effect of flow hysteresis between the open and closed form separations on the turbulence statistics is investigated. We have already observed the time history of the upstream reverse flow area as shown in Fig. 6, where variations of the upstream reverse flow area occur relatively sudden. Here, turbulence statistics by the DNS data is derived by means of conditional averaging based on the sign of dA/dt for the period of $0.3 < A/H^2 < 0.5$ at the streamwise section of $x/H = 0.1$.

Figures 8 and 9 show the profiles of streamwise turbulence intensity and the Reynolds stress, respectively, derived from the conditional averaging based on the sign of dA/dt . From these figures, the effect of flow hysteresis apparently exists. The profiles of the statistics for $dA/dt > 0$ are similar to those for the period of open form separation, while the profiles for $dA/dt < 0$ are similar to those for the period of closed form separation.

Hereafter, turbulence statistics by the DNS is derived by means of conditional averaging based on the upstream reverse flow area at the streamwise section of $x/H = 0.1$ where the CDP of the Reynolds stress is observed. Specifically, the conditional averaging is taken around $A/H^2 = 0.0$ (0.0-0.03), 0.20 (0.19-0.21), 0.40 (0.39-0.41), 0.60 (0.59-0.61), 0.80 (0.79-0.81), and 1.00 (0.99-1.01). Again, $A/H^2 \leq 0.4$ and $A/H^2 \geq 0.5$ correspond to open and closed form separations, respectively.

Figure 10 shows the profiles of streamwise mean velocity at $x/H = 0.1$ derived from the conditional averaging based on the upstream reverse flow area. The amplitude of reverse flow observed close to the upper wall ($y/H = 0.0-0.1$) is greater for open form separation ($A/H^2 \leq 0.4$) than for closed form separation ($A/H^2 \geq 0.5$).

Figure 11 shows the profiles of streamwise turbulence intensity at $x/H = 0.1$ derived from the conditional averaging based on the upstream reverse flow area. The peak value of the intensity around $y/H = 0.1$ is greater for open form separation than for closed form separation, which indicates that the primary peak is produced by the shear layer caused by the step corner. On the other hand, the secondary peak of the intensity appears away from the upper wall ($0.2 < y/H < 0.4$) for closed form separation ($A/H^2 \geq 0.5$), which is produced by the elongated coherent vortex structures get over the step corner.

Figure 12 shows the Reynolds shear stress profiles at $x/H = 0.1$ derived from the conditional averaging based on the upstream reverse flow area. The Reynolds shear stress profiles strongly depend on the upstream reverse flow area. The negative peak value close to the upper wall at $y/H = 0.1$ is greater around the

transition period ($A/H^2 = 0.4-0.6$). The positive peak values at $y/H = 0.15-0.35$ are prominent for $A/H^2 \geq 0.5$. The amplitude of the Reynolds shear stress for the closed form separation ($A/H^2 \geq 0.5$) is much larger than that for the open form separation ($A/H^2 \leq 0.4$).

Figure 13 shows the kinetic energy production profiles at $x/H = 0.1$ derived from the conditional averaging based on the upstream reverse flow area. The negative production of the kinetic energy at $y/H = 0.075$ is prominent when the upstream separation is open, and the amplitude of the negative peak value increases with decreasing the upstream reverse flow area. This implies that the CDP of the Reynolds stress is mainly produced when the upstream separation has open form. Therefore, the negative production and the CDP of the Reynolds stress as well, are produced by the correlation between the shear by the downstream separation and the main stream coherent structures over the forward-facing step.

The production term of the kinetic energy for a two-dimensional mean flow is written as follows:

$$P_k = -\overline{u'^2 \frac{\partial u}{\partial x}} - \overline{u'v' \frac{\partial u}{\partial y}} - \overline{v'^2 \frac{\partial u}{\partial y}} - \overline{u'v' \frac{\partial v}{\partial x}} \quad (2)$$

In this study, the first, second, third, and fourth terms in the right hand side of Eq.(2) are written symbolically as P_{k11n} , P_{k11s} , P_{k22n} , and P_{k22s} , respectively. In the terms, P_{k11s} and P_{k22n} are possible to contribute to the negative production of the kinetic energy as mentioned in Morinishi et al. (2015). The negative production is produced by the combination of negative ($-\overline{u'v'}$) and positive $\partial u/\partial y$ in P_{k11s} , and by positive $\partial v/\partial y$ in P_{k22n} .

Figures 14 (a) and (b) show the mean velocity gradients profiles of $\partial u/\partial y$ and $\partial v/\partial y$ at $x/H = 0.1$, respectively, derived from the conditional averaging based on the upstream reverse flow area. The velocity gradients are positive around $y/H = 0.075$ where the negative production is observed, and they decrease with increasing the upstream reverse flow area.

Figures 15 (a) and (b) show the profiles of P_{k11s} and P_{k22n} at $x/H = 0.1$, respectively, derived from the conditional averaging based on the upstream reverse flow area. The negative production at $y/H = 0.075$ due to the period of open form separation is dominant in P_{k22n} at $x/H = 0.1$, while appreciable difference of P_{k11s} is not observed between the open ($A/H^2 \leq 0.4$) and closed ($A/H^2 \geq 0.5$) form separations. Therefore, in the forward-facing step flow, the production term P_{k22n} in the period of open form separation mainly contribute to the CDP of the Reynolds stress at the section of $x/H = 0.1$.

CONCLUSION

The turbulence structure of the Couette flow with a forward-facing step is studied using PIV and DNS. The conditional averaging based on the reverse flow area (A) in the upstream separation is introduced to distinguish the form of the upstream separation. The upstream separation has open form when $A/H^2 \leq 0.4$, while it has closed form when $A/H^2 \geq 0.5$. The open form separation reattaches on the forward-facing step, while the closed form separation gets over the step corner and encloses the downstream separation. In addition, the effect of flow hysteresis between the open and closed form separations exists on the turbulence statistics. The counter-gradient diffusion phenomena

(CDP) of the Reynolds stress appeared near the downstream separation is then analysed by means of the conditional averaging based on the reverse flow area. The CDP of the Reynolds stress is mainly produced when the upstream separation is open form.

ACKNOWLEDGEMENT

We are grateful to Mr. Yoshikawa and Mr. Yamamoto for their assistance with the experimental measurements.

REFERENCES

- Hattori, H. and Nagano, Y., 2010, "Investigation of turbulent boundary layer over a forward-facing step via direct numerical simulation", *Int. J. Heat and Fluid Flow*, Vol. 31, pp. 284-294.
- Morinishi, Y., Yoshikawa, D., and Tamano, S., 2015, "Counter-gradient diffusion of Reynolds stress in turbulent Couette flow with forward-facing step", *Proceedings, European Turbulence Conference 15*, USB (2p).
- Pearson, D. S., Goulart, P. J., and Ganapathisubramani, B., 2013, "Turbulent separation upstream of a forward-facing step", *J. Fluid Mech.*, Vol. 724, pp. 284-304.

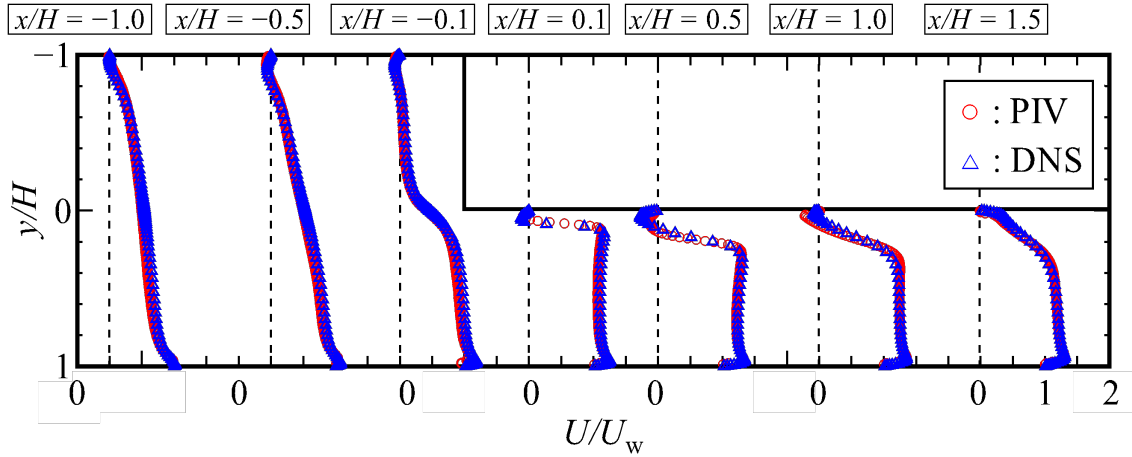


Figure 2. Streamwise mean velocity profiles at several downstream sections. These data are estimated by means of standard ensemble averaging. Red circles : PIV measurement, Blue triangulars : DNS result.

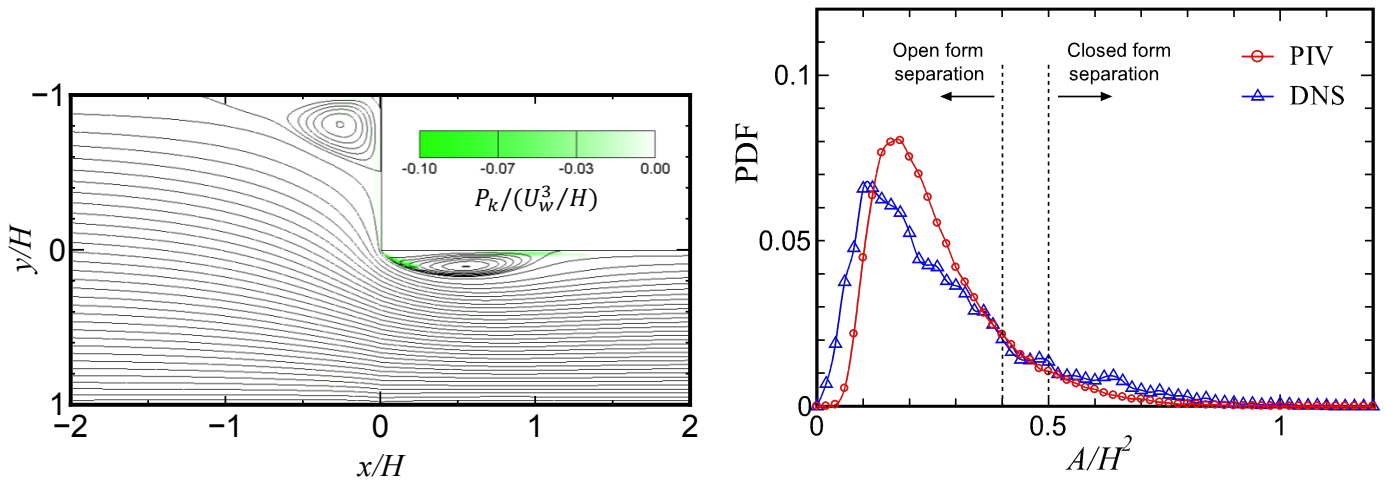
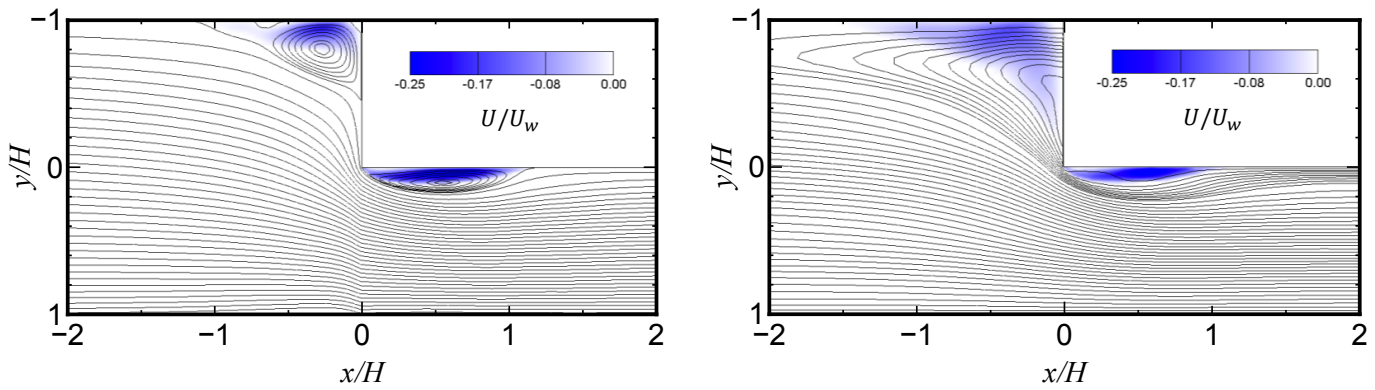


Figure 3. Streamlines and negative production regions (green) of turbulence kinetic energy computed from DNS.

Figure 4. Probability density function of reverse flow area in upstream separation region.



(a) Open form separation ($A/H^2 = 0.19 - 0.21$)

(b) Closed form separation ($A/H^2 = 0.59 - 0.61$)

Figure 5. Streamlines and reverse flow regions (blue) corresponding to the upstream reverse flow area computed from DNS.

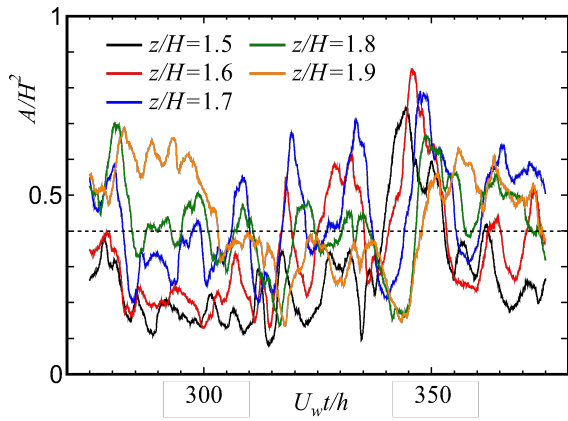
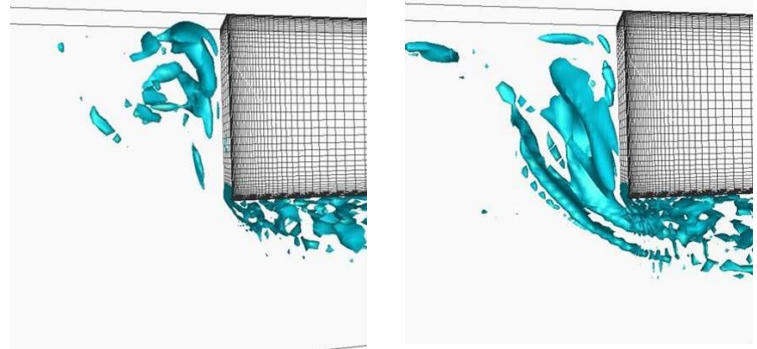


Figure 6. Time history of the upstream reverse flow area at some spanwise sections.



(a) $U_w t/H = 314$ (b) $U_w t/H = 350$

Figure 7. Isosurface of $Q_2 H^2 / U_w^2 = 1.0$.

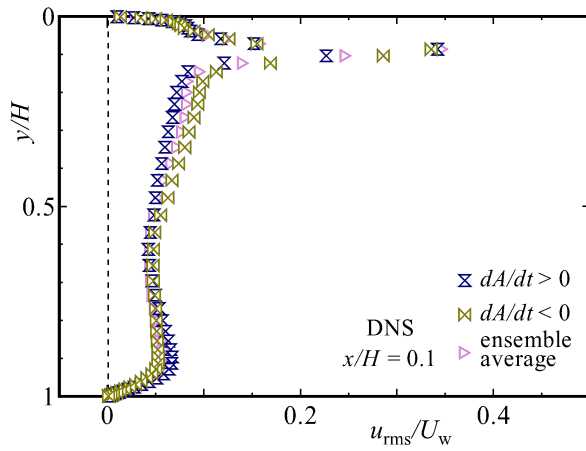


Figure 8. Profiles of streamwise turbulence intensity at $x/H = 0.1$ corresponding to the variation sign of the upstream reverse flow area.

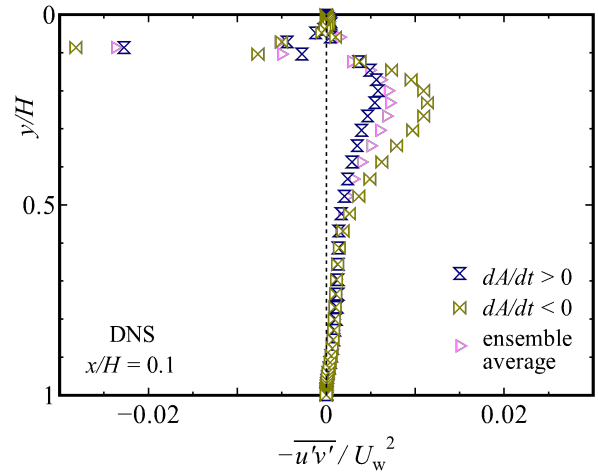


Figure 9. Profiles of Reynolds stress at $x/H = 0.1$ corresponding to the variation sign of the upstream reverse flow area.

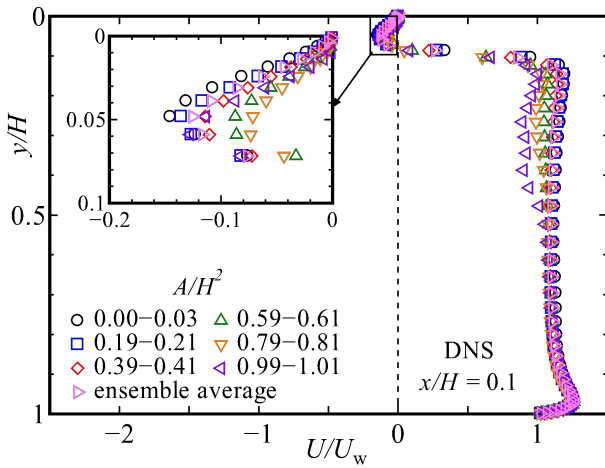


Figure 10. Profiles of streamwise mean velocity at $x/H = 0.1$ corresponding to the upstream reverse flow area computed from DNS.

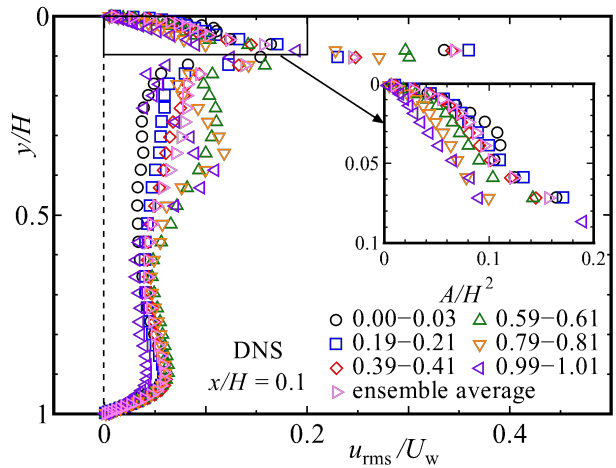


Figure 11. Profiles of streamwise turbulence intensity at $x/H = 0.1$ corresponding to the upstream reverse flow area computed from DNS.

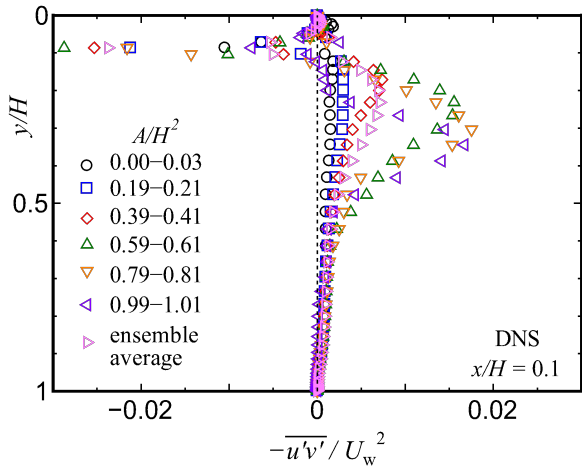


Figure 12. Profiles of the Reynolds shear stress at $x/H = 0.1$ corresponding to the upstream reverse flow area computed from DNS.

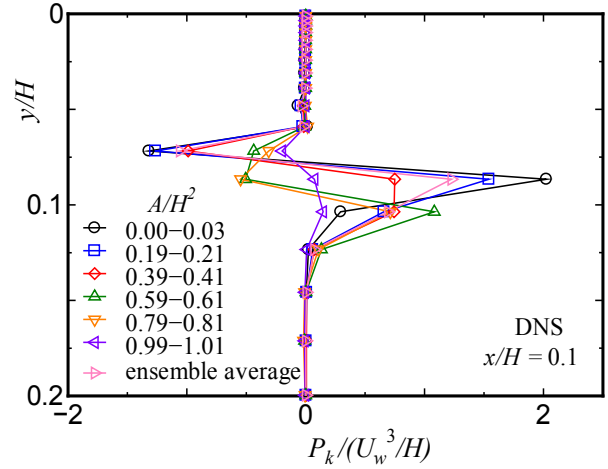
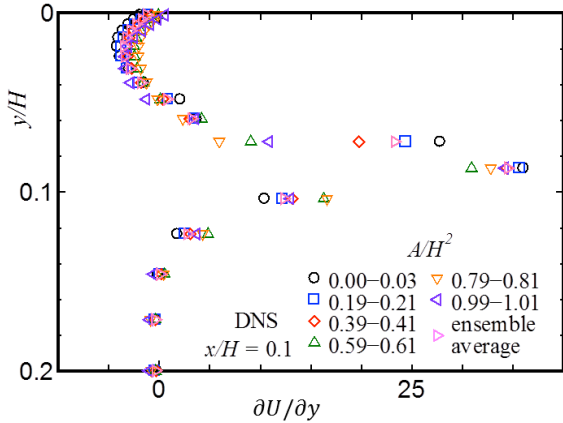
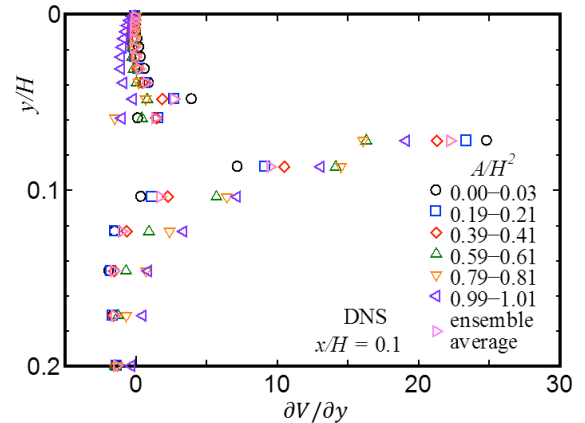


Figure 13. Profiles of the turbulence kinetic energy production at $x/H = 0.1$ corresponding to the upstream reverse flow area computed from DNS.

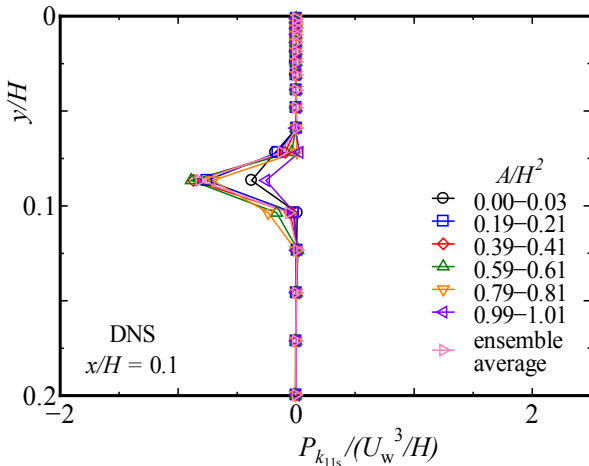


(a) $\partial U / \partial y$

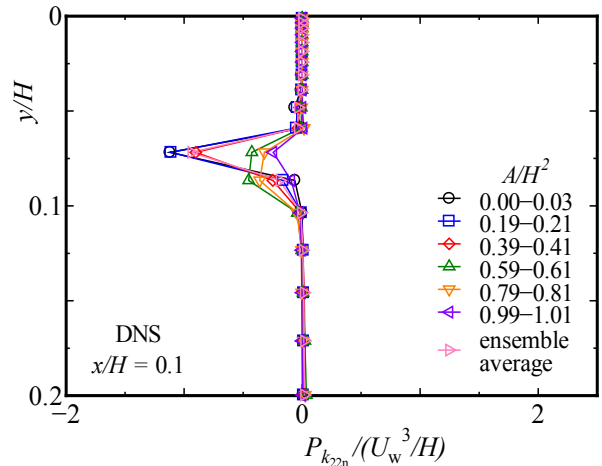


(b) $\partial V / \partial y$

Figure 14. Profiles of mean velocity gradient at $x/H = 0.1$ corresponding to the upstream reverse flow area computed from DNS.



(a) $P_{k_{11s}}$



(b) $P_{k_{22n}}$

Figure 15. Profiles of $P_{k_{11s}}$ and $P_{k_{22n}}$ at $x/H = 0.1$ corresponding to the upstream reverse flow area computed from DNS.